

Terra rossa as the substrate for biological phosphate removal from wastewater

G. DURN¹, J. HRENOVIC^{2,*} AND L. SEKOVANIC³

¹ University of Zagreb, Faculty of Mining, Geology and Petroleum Engineering, Pierottijeva 6, Zagreb, Croatia,

² University of Zagreb, Faculty of Science, Division of Biology, Rooseveltov trg 6, Zagreb, Croatia, and ³ University of Zagreb, Geotechnical Faculty, Hallerova aleja 7, Varazdin, Croatia

(Received 27 June 2013; revised 30 October 2013; Editor: George Christidis)

ABSTRACT: Three samples of terra rossa were shown to be efficient adsorbents of phosphate [P(V)] from wastewater and removed 29.9–32.6% of P(V). The total iron content in terra rossa was the key factor which determined the P(V) removal from wastewater. The original samples of terra rossa were effective support materials for the immobilization of metabolically active P(V)-accumulating bacteria *Acinetobacter junii* ($0.56\text{--}2.47 \times 10^{10}$ CFU g⁻¹). The removal of oxalate-extractable iron from original sample of terra rossa increased the number of immobilized bacteria to 1.34×10^{11} CFU g⁻¹, which is the largest number of immobilized bacteria reported in the literature so far. In reactors containing the *A. junii* and terra rossa P(V) was removed from wastewater by simultaneous adsorption onto terra rossa and accumulation inside bacterial cells, resulting in 40.5–62.5% of P(V) removal. Terra rossa is a promising substrate for biological P(V) removal from wastewater, acting both as adsorbent of P(V) and carrier of P(V)-accumulating bacteria.

KEYWORDS: bacteria, immobilization, phosphate, sorption isotherm, terra rossa, wastewater.

The discharge of excessive volumes of phosphate P(V)-containing wastewaters into closed water bodies results in eutrophication of aquatic ecosystems. Eutrophication significantly changes water quality and reduces the quality of surface waters for human use. Therefore, there is need to remove P(V) from municipal and industrial wastewaters before its discharge into natural recipients. Several methods have been used for removal of P(V) from wastewater, among which the adsorption and biological P(V) removal have been widely studied. Various natural and synthetic materials and industrial by-products rich in Ca, Fe or Al have been tested for P(V) adsorption in aqueous media (e.g. Mortula *et al.*, 2007; Li *et al.*, 2013), among which, dewatered alum and ferric alum sludge have been reported as some of the most efficient P(V)

adsorbents with P(V) adsorption capacities ranging from 0.7 to 45 mg P(V) g⁻¹ (Mortula *et al.*, 2007; Wang *et al.*, 2011). Al-rich materials such as alum sludge are not environmentally friendly due to leaching of toxic Al species. Moreover, many of the tested materials influence the neutral pH values of treated water. The ideal material for P(V) removal from wastewaters should be inert, nontoxic, cheap, widely available and useful for soil amendment after saturation with P(V).

The biological P(V) removal from wastewaters is carried out by P(V)-accumulating bacteria. These bacteria are effective in P(V) removal from wastewater by the transport of extracellular present soluble P(V) into the cell and its conversion to insoluble intracellular poly-P(V) (Sidat *et al.*, 1999). Currently attention is paid to the immobilization of P(V)-accumulating bacteria onto suitable materials in order to achieve a higher cell density in bioreactors, and as a result, greater efficiency of wastewater treatment process (e.g. Hrenovic *et al.*,

* E-mail: jasna.hrenovic@biol.pmf.hr
DOI: 10.1180/claymin.2013.048.5.05

2009a,b, 2010, 2012). Due to its inertness and high Fe content terra rossa is a promising material for adsorption of P(V) and immobilization of P(V)-accumulating bacteria.

Terra rossa is a reddish clayey to silty/clayey soil developed over limestones and dolomites; it is especially widespread in the Mediterranean region. Its bright red colour is a diagnostic feature and results from the preferential formation of hematite over goethite, known as rubification. The rather limited extent of variation of selected Fe-oxide characteristics may indicate a specific pedo-environment in which terra rossa is formed (Boero & Schwertmann, 1989). Terra rossa has a slightly alkaline to neutral pH and high base saturation with calcium and/or magnesium as dominant cations. It is well drained because it is well aggregated (high content of exchangeable Ca and Mg) and it is situated on highly permeable carbonate rocks (Torrent, 1995). Terra rossa is formed as a result of (1) decalcification, (2) rubification and (3) bisiallization and/or monosiallization (Durn *et al.*, 1999). The clay mineral composition of terra rossa in the Mediterranean may be very variable and consists of kaolinite, illite, hydroxy-interlayered vermiculite and smectite (e.g. Moresi & Mongelli, 1988; Garcia-Gonzales & Recio, 1988; Boero *et al.*, 1992; Atalay, 1997; Bronger & Bruhn-Lobin, 1997; Durn *et al.*, 1999). In Soil Taxonomy (Soil Survey Staff, 1975), terra rossas are classified as Alfisols (Haploxeralfs or Rhodoxeralfs), Ultisols, Inceptisols (Xerochrepts) and Mollisols (Argixerolls or Haploxerolls). According to the UN Food and Agriculture Organisation system (FAO, 1974) terra rossa soils are recognized as Luvisols (Chromic Luvisols), Phaeozems (Haplic Phaeozems or Luvic Phaeozems) and Cambisols. In other classification systems using Mediterranean climate as the major soil differentiating criterion, the term terra rossa is used to describe the soil subclass "Modal Fersiallitic Red soil" when situated on limestones (Duchaufour, 1982). Several national soil classifications (e.g. Croatia, Italy, Israel) retain the term "terra rossa" for limestone-derived red soils. Different authors have considered terra rossa to be a soil, vetusol, relict soil (non-buried-palaeosol), palaeosol or pedo-sedimentary complex. However, most workers consider terra rossa a polygenetic relict soil, formed during the Tertiary and/or hot and humid periods of the Quaternary (e.g. Altay, 1997; Bronger & Bruhn-Lobin, 1997; Durn *et al.*, 1999). Based on new field and petrographic evidence Merino &

Banerjee (2008) proposed a new theory of terra rossa formation through replacement of limestone by authigenic clay at a narrow reaction front; they explained why terra rossa and karst are associated. Banerjee & Merino (2011) successfully modelled the new terra rossa-forming process quantitatively and compared model-calculated rates of formation of terra rossa to rates obtained palaeomagnetically.

Terra rossa is the most widespread soil type in Istria, Croatia, a region that has been affected by karst processes, (neo)tectonic activity and sediment supply since the Late Tertiary (Durn *et al.*, 2007). Durn *et al.* (1999) presented evidence for the polygenetic nature of terra rossa in Istria, based on detailed mineralogical and geochemical investigations. The clay fraction of terra rossa from Istria contains both hematite and goethite (Durn *et al.*, 2001). The size of hematite crystals is less than 50 nm which is in accordance with values reported by Boero & Schwertmann (1989). The mean values of Fe_t (total iron), Fe_d (iron extractable with Na dithionite-citrate bicarbonate, i.e. iron extracted from all Fe oxides) and Fe_o (iron extractable with ammonium oxalate, i.e. iron extracted only from poorly crystalline Fe oxides) in Istrian terra rossa are 5.19, 3.68 and 0.39%, respectively, and the mean value of the Fe_d/Fe_t ratio is 0.7 (Durn *et al.*, 2001). Poorly crystallized kaolinite, which does not form intercalation compounds with dimethylsulfoxide (DMSO) is the dominant mineral phase in the fine clay of terra rossa and is considered predominantly authigenic (pedogenic) rather than being inherited from parent materials (Durn *et al.*, 1999).

Terra rossa in Istria has high kaolinite and illite contents (Durn *et al.*, 1999). It fills cracks and sinkholes, and forms a discontinuous surface layer up to 2.5 m thick. Thick, up to 14 m accumulations of terra rossa-like material are found in karst depressions, in the form of colluvial pedo-sedimentary complexes which are used as raw materials for the brick industry. The aim of the present contribution is to test terra rossa as a substrate for the improvement of biological P(V) removal from wastewater.

MATERIALS AND METHODS

Characterization of terra rossa

Terra rossa samples from B horizons formed on limestone of Cretaceous age were collected at three localities in Istria, Croatia (sample 3686 Pomer;

sample 3687 Savudrija and sample 3688 Novigrad). These locations represent typical sites for terra rossa and were selected from 16 terra rossa sampling locations studied in a previous work (Durn *et al.*, 1999). Samples were air-dried after crushing the aggregates by hand and were passed through a 2 mm sieve. Particle size analysis was carried out on the <2 mm fraction after dispersion in water and ultrasonic treatment. Fractions >45 µm were obtained by wet sieving. The <2 µm and 2–10 µm fractions were separated by sedimentation in cylinders following Stokes law and were determined quantitatively. The remaining portion in the cylinders was treated as the 10–45 µm fraction. For the experiments with bacteria and P(V) removal from wastewater the <100 µm fraction obtained by wet sieving was used. This fraction generally represents >99 wt.% of analysed samples (Table 1).

Major and trace elements in terra rossa (fraction <2 mm) were measured with an X-ray fluorescence (XRF) spectrometer (Philips PW 1404) using pressed powder pellets. Iron and manganese extractable with Na dithionite-citrate bicarbonate (Fe_d, Mn_d) were extracted according to Mehra & Jackson (1960) and were measured by atomic absorption spectroscopy (AAS, Pye-Unicam SP9). This treatment extracts practically all secondary Fe oxides (Schwertmann & Taylor, 1989). Iron and manganese were extracted with ammonium oxalate (Fe_o, Mn_o) according to Schwertmann (1964) and determined with AAS. Acid ammonium oxalate extracts only poorly crystalline Fe oxides, predominantly ferrihydrite (Schwertmann, 1964; Schwertmann *et al.*, 1982; Schwertmann & Taylor, 1989). In order to test the influence of iron oxides on the experiments with bacteria and P(V) removal from wastewater, three samples were produced from sample 3686 (fraction <100 µm). In sample 3686_o Fe_o (poorly crystalline Fe oxides) was removed, whereas in sample 3686_d Fe_d (practically all secondary Fe oxides) was removed.

The mineralogical composition of the <2 mm and <2 µm fractions of terra rossa was determined by X-ray powder diffraction (XRD) using a Philips diffractometer (graphite monochromator, Cu-Kα radiation, proportional counter). Before the analysis of the clay fraction, humic materials and iron oxides were removed according to Tributh & Lagaly (1986) and Tributh (1991). Coarse and medium clay fractions (2–0.2 µm) and the fine clay fraction (<0.2 µm) were also examined by XRD after quantitative separation from the <2 µm

TABLE 1. Particle size analysis (wt.%), total iron (wt.%), dithionite and oxalate extractable iron (wt.%) and manganese (ppm) of the terra rossa samples (<2 mm).

Sample	Clay	Silt	Sand*	Fe _t	Fe _d	Fe _o	Fe _d /Fe _t	Fe _o /Fe _d	Mn _t	Mn _d	Mn _o	Mn _d /Mn _t	Mn _o /Mn _d
3686	70.2	28.7	1.1	5.60	3.91	0.38	0.70	0.10	930	662	512	0.71	0.77
3686 _o **				5.22									
3686 _d ***				1.69									
3687	42.1	55.3	2.5	5.47	3.76	0.30	0.69	0.08	387	287	87	0.74	0.30
3688	77.2	21.9	0.9	6.51	4.90	0.36	0.75	0.07	775	477	308	0.62	0.65

Clay (<2 µm), silt (2–63 µm) and sand (>63 µm*). Total iron in sample 3686_o** is Fe_t-Fe_o. Total iron in sample 3686_d*** is Fe_t-Fe_d. * wt.% of size fractions >100 µm in samples 3686, 3687 and 3688 are 0.04, 1.09 and 0.52 respectively.

fraction. The XRD patterns of random samples were obtained after the following treatments: (a) air-drying and (b) dissolution in HCl (1:1). The XRD patterns of oriented samples were obtained after the following treatments: (a) air drying, (b) ethylene glycol solvation, (c) Mg-saturation, (d) K-saturation, (e) Mg-saturation and ethylene glycol solvation, (f) Mg-saturation and glycerol solvation, (g) K-saturation and DMSO solvation, and (h) heating for two hours at 550°C.

The identification of clay minerals was generally based on the methods outlined by Brown (1961), Brindley & Brown (1980) and Moore & Reynolds (1989). The term "illitic material" was used as defined by Środoń (1984) and Środoń & Eberl (1984). The term "low-charge vermiculite or high-charge smectite" refers to clay minerals which were found only in the <0.2 µm fraction and have some typical properties of both smectites and vermiculites (Ruhlicke & Niederbudde, 1985; Douglas, 1989). The term "MC" was used for mixed-layer clay mineral(s), in which type of interstratification and constituting clay minerals were not recognized with certainty. The DMSO-treatment enabled the differentiation of kaolinities which form intercalation compounds with DMSO (Kl_D) from kaolinities which do not intercalate with DMSO (Kl) (Range *et al.*, 1969). Magnesium-saturated ethylene glycol and glycerol-solvated samples were used to detect vermiculite in cases where smectite is also present in the sample (Douglas, 1989).

The amounts of quartz, plagioclase and K-feldspar were determined by means of semi-quantitative XRD analysis. An external standard was applied, by measuring relative intensities of characteristic diffraction lines. Estimation of iron oxide percentages (hematite + goethite) was based on the iron content, which was extractable with Na dithionite-citrate bicarbonate. The term "iron oxide" includes oxides, oxyhydroxides and hydrated oxides according to Schwertmann & Taylor (1989). Semiquantitative estimates of clay minerals in the 2–0.2 µm and <0.2 µm fractions were based on the intensities of characteristic X-ray peaks following the method of Johns *et al.* (1954) and using multiplication factors given by Riedmuller (1978).

Phosphate sorption isotherms

Air-dried original and modified samples of terra rossa 3686 (0.2 g, fraction <100 µm) were shaken (70 rpm) for 24 h at 25°C with 20 mL of 0.1 M KCl

solution containing 2 to 50 mg P(V) L⁻¹ as KH₂PO₄ with one drop of chloroform to inhibit the growth of microorganisms. The pH value was adjusted to 7.00±0.04 with 1 M NaOH or 1 M HCl (Kemika, Croatia). After equilibration had been achieved the suspension was centrifuged at 4000 rpm for 10 min. The phosphate (P-PO₄³⁻) concentration in the supernatant was measured spectrophotometrically with a DR/2500 Hach spectrophotometer using the molybdovanadate method (Hach method 8114). The P(V) sorption efficiency by terra rossa was calculated using equation 1:

$$P(V) (\%) = [(Ca_o - C)/Ca_o] \cdot 100 \quad (1)$$

In the retention stage, the solid concentration at equilibrium is given by equation 2

$$Q = (Ca_o - C) \cdot (V/m) + Qa_o \quad (2)$$

where Ca_o and C (mg L⁻¹) are the initial and equilibrium mass concentrations of P(V), respectively; V (L) is the volume of the P(V) solution; m (g) is the mass of dry adsorbent terra rossa used; Qa_o (mg g⁻¹) is the mass concentration of P(V) initially retained by terra rossa and Q (mg g⁻¹) is the amount of P(V) adsorbed by terra rossa at equilibrium.

The equilibrium adsorption data were analysed according to the linear form of exponential Freundlich [equation 3] and parabolic Langmuir [equation 4] isotherm models (Limousin *et al.*, 2007):

$$\ln Q = (1/n) \cdot \ln C + \ln (K_F) \quad (3)$$

and,

$$(C/Q) = (1/Q_{\max}) \cdot C + 1/(Q_{\max} \cdot L) \quad (4)$$

where Q (mg g⁻¹) is the amount of P(V) adsorbed by terra rossa at equilibrium; K_F (L g⁻¹) and n (dimensionless) are two Freundlich isotherm constants; C (mg L⁻¹) is the residual P(V) mass concentration in the solute after equilibration; Q_{\max} (mg g⁻¹) is the maximum sorption capacity; constant L (L mg⁻¹) corresponds to the affinity between the sorbate and sorbent.

The Freundlich isotherm assumes the heterogeneity of the surface as well as multilayer sorption, interaction between the adsorbed molecules and the exponential distribution of active sites and their energies. According to the Freundlich equation, the isotherm does not reach a plateau as C increases. A graph with $\ln C$ vs. $\ln Q$ provides a

line of slope $k = 1/n$ and intercepts $I = \ln(K_F)$. Values of $n > 1$ represent favourable adsorption conditions. The Langmuir isotherm is based on the three key assumptions; monolayer coverage, site equivalence and site independence. A plot of C/Q against C should give a straight line with slope $k = 1/Q_{\max}$ and intercept $I = 1/(Q_{\max} \cdot L)$. The dimensionless (R_L) adsorption intensity (Sawahl *et al.*, 2006) is calculated from equation 5:

$$R_L = 1/(1 + L \cdot Ca_o) \quad (5)$$

where Ca_o is the initial solute concentration and L is the Langmuir adsorption constant. The average value of R_L indicates that adsorption is unfavourable ($R_L > 1$), linear ($R_L = 1$), favourable ($0 < R_L < 1$) or irreversible ($R_L = 0$).

Experiments with bacteria and phosphate removal from wastewater

The $<100 \mu\text{m}$ fraction of dry terra rossa samples was sterilized by autoclaving at 121°C for 15 min. The culture of P(V)-accumulating bacteria *A. junii* strain DSM 1532 was obtained from the Deutsche Sammlung von Microorganismen und Zellkulturen GmbH. A chemically defined water solution was used to simulate the real wastewater. The composition was as follows (in mg L^{-1} of distilled water): Na-propionate 300; peptone 100; MgSO_4 10; CaCl_2 6; KCl 30; yeast extract 10; KH_2PO_4 88. The P(V) concentration was 20 mg L^{-1} in order to accurately follow the P(V) removal. The pH value was adjusted to 7.00 ± 0.04 with 1 M NaOH or 1 M HCl before autoclaving ($121^\circ\text{C}/15 \text{ min}$).

For the experiments (Fig. 1) the bacteria *A. junii* was pre-grown on a nutrient agar (Biolife, Italy) for

16 h at $30 \pm 0.1^\circ\text{C}$. The biomass was then suspended in sterile 0.05 M NaCl solution. One mL of suspended biomass was inoculated into bottles containing 100 mL of synthetic wastewater. An amount of 1.0 g of terra rossa was added to each bottle. The control bottle was left without addition of terra rossa. The bottles were sealed with a sterile gum cap and aerobically incubated in a water bath with shaker ($30 \pm 0.5^\circ\text{C}/70 \text{ rpm}$, Memmert WNB) for 24 h. Filtered air was provided at an aeration rate of 1 L min^{-1} . In order to determine the P(V) removal only by terra rossa, the same experiment was performed without addition of bacteria.

The pH-value was measured with a WTW 330 pH meter. The phosphate (P-PO_4^{3-}) concentration in the synthetic wastewater was measured spectrophotometrically with a DR/2500 Hach spectrophotometer using the molybdovanadate method (Hach method 8114). Before the P(V) measurement the samples were filtered with $0.2 \mu\text{m}$ Sartorius nitrocellulose filters. The number of planktonic and immobilized bacteria were measured at the beginning and after 24 h of experiment. For the determination of planktonic bacteria, 1 mL of supernatant was serially diluted (10^{-1} to 10^{-9}) and volumes of 0.1 mL were aseptically inoculated onto the nutrient agar (spread plate method). After the incubation ($30 \pm 0.1^\circ\text{C}/24\text{h}$), the bacterial colonies were counted and the number of viable cells was reported as colony-forming units (CFU) mL^{-1} . To determine the number of immobilized cells, each carrier was taken from the flask, washed three times with sterile 0.05 M NaCl solution, and aseptically placed into a tube containing 9 mL of 0.05 M NaCl. The samples were crushed with a sterile glass rod and vigorously shaken on a

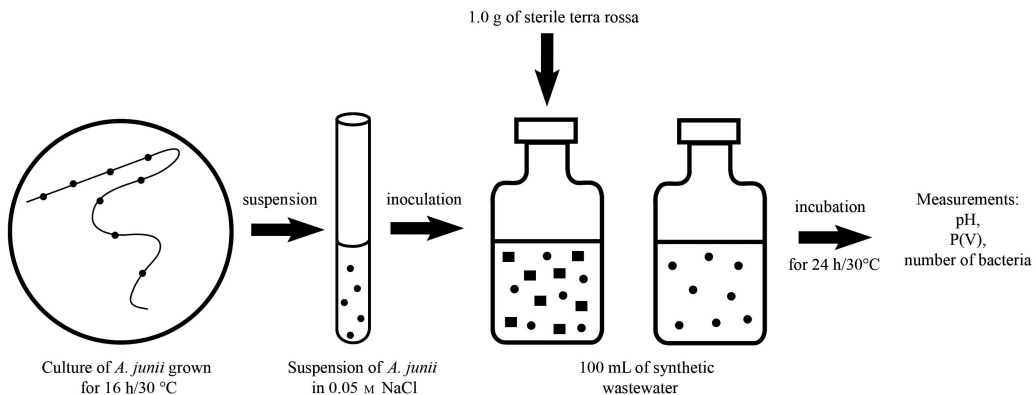


FIG. 1. Schematic illustration of experimental design used to test P(V) removal from wastewater.

mechanical shaker (40 Hz/3 min, Kartell TK3S). This procedure detaches immobilized cells from the carrier (Durham *et al.*, 1994). Serial dilutions were made from these suspensions and nutrient agar plates were inoculated and incubated as already described. After the incubation the colonies were counted and the remaining samples were dried and weighed. The number of cells was reported as immobilized CFUs.g⁻¹ of dry terra rossa. All measurements were done in triplicate.

Statistical analyses were carried out using Statistica Software 9.1 (StatSoft, Tulsa, USA). The numbers of bacterial CFU were logarithmically transformed beforehand to normalize distribution and to equalize variances of the measured parameters. The comparisons between samples were done using the one-way analysis of variance (ANOVA) and subsequently the post-hoc Duncan test was performed for the calculations concerning pair-wise comparisons. The correlation between variables was estimated by Pearson linear correlation analysis. Statistical decisions were made at a significance level of $p < 0.05$.

RESULTS AND DISCUSSION

Characterization of terra rossa

Terra rossa samples are composed mainly of clay (<2 µm) and silt-sized (2–63 µm) particles, with sand (>63µm) particles being less than 3 wt.% (Table 1). Samples 3686 and 3688 are characterized as clays while sample 3687 is silty clay according to the Soil Survey Staff (1975). The wt.% of the >100 µm size fractions in samples 3686, 3687 and 3688 are 0.04, 1.09 and 0.52 respectively.

The Fe_d/Fe_t ratio, which is considered as an index of weathering (Bech *et al.*, 1997), varies from 0.69 to 0.75, and reflects extensive weathering of Fe-containing primary silicates (Table 1), suggesting that hematite and goethite are the main

iron-containing phases. Clay, Fe_t and Fe_d contents are correlated, suggesting a connection of Fe oxides with the clay fraction (Table 1). Low values of Fe_o point to the low content of poorly crystalline Fe oxides (probably ferrihydrite) in analysed terra rossa. This was expected because most of the Fe oxides in fersialitic soils are crystallized (Bech *et al.*, 1997). Mn_d/Mn_t ratio varies in analysed samples from 0.62 to 0.74 (Table 1), indicating that most of the manganese in analysed terra rossa samples is in the form of Mn oxides and hydroxides. The values of Mn_o are lower compared to those of Mn_d. However, the Mn oxides and hydroxides in soil should be associated with Mn_d rather than Mn_o, which does not provide additional qualitative information (Blume & Schwertmann, 1969).

Terra rossa samples contain quartz, plagioclase, K-feldspar, micaceous clay minerals (illitic material and mica), kaolinites (Kl_D and Kl), chlorite, vermiculite, low-charge vermiculite or high-charge smectite, mixed-layer clay minerals (other than illitic material), hematite, goethite and XRD-amorphous inorganic compound (Tables 2–4). The amount of quartz is highest in the silt-dominated sample (3687). Main mineral phases in the clay fraction of analysed terra rossa samples are kaolinite (Kl_D and Kl), illitic material, Fe-oxides and XRD amorphous inorganic compounds, while vermiculite, low-charge vermiculite or high-charge smectite, chlorite, mixed-layer clay minerals and quartz are present sporadically in subordinate amounts (Tables 3 and 4; Fig. 2). The coarse and medium clay fraction contains both kaolinites while kaolinite Kl which does not form intercalation compounds with DMSO is the dominant mineral phase in the fine clay (Table 4). Low-charge vermiculite or high-charge smectite was detected only in the fine clay of sample 3687. The chemical composition of terra rossa samples is very similar (Tables 5 and 6). The sample 3688 with the highest amount of clay fraction (Table 1) and kaolinite

TABLE 2. Mineralogical composition of the <2 mm fraction of terra rossa (wt.%).

Sample	Quartz	Plagioclase	K-feldspar	Hematite+goethite	Phyllos.+am.
3686	21	2	1	6	70
3687	29	1	1	5	64
3688	15	1	1	7	76

Phyllos.+am. = Phyllosilicates and amorphous inorganic compounds.

TABLE 3. Mineralogical composition of the <2 µm fraction of terra rossa after the removal of carbonates, humic materials and iron oxides.

Sample	Illitic material	KI _D	KI	Vermiculite	L.c. vermiculite	Chlorite	Mc	Quartz
3686	+	+	+	+			+	+
3687	+	+	+	+	x	+	+	+
3688	+	+	+	+			+	+

KI_D = Kaolinite which forms intercalation compounds with DMSO, KI = Kaolinite which does not intercalate with DMSO, L.c. vermiculite = Low-charge vermiculite or high-charge smectite, Mc-Mixed-layer clay mineral, x = present only in the <0.2 µm fraction.

(Tables 2–4) has the highest Al₂O₃, Fe₂O₃ and LOI, and the lowest Na₂O, MgO and K₂O contents. The abundance of trace elements in analysed samples is comparable with that in cambisols and luvisols developed on carbonate rocks in the Istrian region (Miko *et al.*, 1999, 2001, 2003). Higher content of Cr, V and Co in analysed samples compared to regional means (Miko *et al.*, 2001) can be attributed to high sorption capacity of iron and manganese oxides in terra rossa and their affinity for these metals.

Phosphate sorption isotherms

Experimental results of P(V) sorption from a solution of P(V) salt by original and modified samples of terra rossa 3686 are listed in Table 7. The Q_{a_0} values for P(V) initially retained by terra

rossa samples 3686 (9.8×10^{-4}), 3686_o (3.3×10^{-4}) and 3686_d (3.3×10^{-4}) were very small and therefore Q_{a_0} was neglected in equation 2. The differences in P(V) adsorption capacity for all three samples were small and cannot only be attributed to the removal of the Fe-oxides in treatment with oxalate and dithionite. The removal of Fe-oxides increased the concentration of the free active adsorptive sites on disaggregated colloidal particles of kaolinite and illite, which is reflected in the small differences in adsorption capacity of samples 3686, 3686_o and 3686_d. The P(V) sorption maxima (Q_{max}) of kaolin (Muljadi *et al.*, 1966) ranged from 0.76–1.39 mg P(V) g⁻¹ and are comparable to this study. The high Q_{max} values can be explained by the small crystal size, large surface area, and high population of Fe-OH and Al-OH sites where P(V) sorption might occur. Terra rossa contains highly

TABLE 4. Semiquantitative clay mineral composition of the < 0.2 µm and 2–0.2 µm fractions of terra rossa after the removal of carbonates, humic materials and iron oxides.

Sample	Illitic material	KI _D	KI	Vermiculite	l.c. vermiculite	Chlorite	Mc
<0.2 µm							
3686	30		70	tr.			+
3687	10		77	tr.	13		+
3688	19		78	3			+
2–0.2 µm							
3686	44	12	35	9			+
3687	50	12	33	5		tr.	+
3688	35	10	43	12			+

KI_D = Kaolinite which forms intercalation compounds with DMSO, KI = Kaolinite which does not intercalate with DMSO, L.c. vermiculite = Low-charge vermiculite or high-charge smectite, Mc-Mixed-layer clay mineral, Ch/V = chlorite/vermiculite, Illitic material+KI_D+ KI+Vermiculite+L.c. vermiculite+chlorite = 100 wt.%.

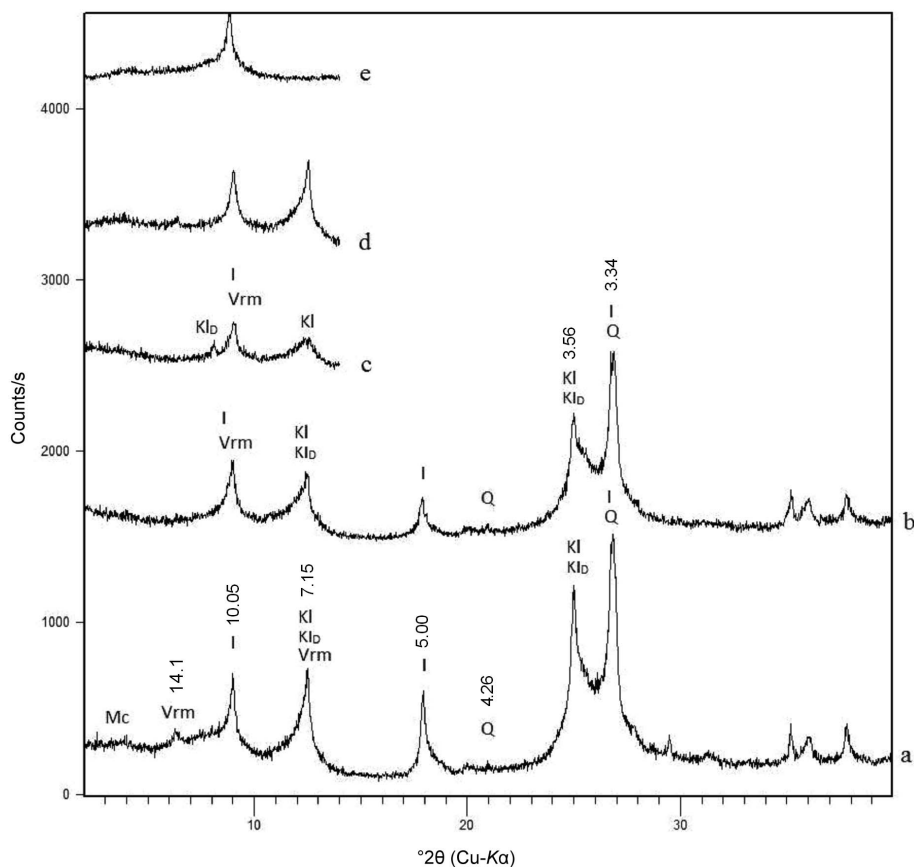


FIG. 2. The XRD patterns of terra rossa sample 3686 (<2 μm fraction) after removal of humic materials and Fe oxides; a,b,c,d,e – oriented samples: (a) Mg-saturated; (b) K-saturated; (c) K-saturated and DMSO solvated; (d) Mg-saturated and glycerol treated; (e) heated for 2 h at 550°C. Vrm: Vermiculite. MC: mixed-layer clay mineral. I: Illitic material. Kl_D : Kaolinite which intercalates with DMSO. Kl: Kaolinite which does not intercalate with DMSO. Q: Quartz. *d* values (in Å) of important peaks are indicated.

heterogeneous surfaces and a variety of adsorption sites on the kaolinite, illite and Fe-oxides. The samples 3686, 3686_b and 3686_d can be considered as kaolinite-hematite systems with reactive amphoteric pH-dependent sorption sites. The hydroxyl groups (silanol and aluminol, -SiOH, -AlOH) at the edges are the major reactive sites on the clay surfaces. The fraction of edge surfaces for kaolinite is 12–14% (Sondi & Pravdic, 1998).

The parameters in Table 8 show that the adsorption can be described well with both Freundlich and Langmuir isotherms; the coefficient of determination R^2 is 0.90–0.99, which suggests monolayer adsorption of P(V) on the solid/liquid interfaces. The relatively low R^2 value (0.90)

obtained from the linear Langmuir isotherm equation for sample 3686_d indicates irregularities and heterogeneity on the outer surface which clearly deviates from the important Langmuir condition of adsorption site equivalence. The adsorption isotherms fitted better with the Freundlich exponential equation in the case of rigorous analysis based on the value of R^2 obtained. The Freundlich model also considers that the sites with strong affinity for P(V), such as the most active sites $\equiv\text{Fe-OH}$ on terra rossa, are occupied first (Davis *et al.*, 2003). The high values of dimensionless Freundlich constant n (2.69–3.59) for the linear $\ln(Q)$ vs. $\ln(C)$ plots indicate a strong bond between the adsorbent terra rossa and P(V).

TABLE 5. Major elements concentrations (wt.%) and dry colour after Munsell Soil Color Charts (1994) of the terra rossa samples.

Sample	Colour	SiO ₂	TiO ₂	Al ₂ O ₃	Fe ₂ O ₃	MnO	MgO	CaO	Na ₂ O	K ₂ O	P ₂ O ₅	LOI	Sum
3686	10R4/8	51.98	1.12	22.01	8.01	0.12	1.09	0.50	0.93	2.19	0.16	11.68	99.94
3687	2.5YR4/8	57.97	1.08	18.42	7.82	<0.05	1.13	1.04	0.23	1.66	0.09	10.78	100.32
3688	2.5YR4/6	47.91	1.01	23.39	9.31	0.10	0.85	0.64	0.18	1.55	0.12	14.82	99.93

The calculated values of the average dimensionless separation factors $R_L(3686) = 0.22$, $R_L(3686_o) = 0.30$ and $R_L(3686_d) = 0.39$ suggest that the adsorption was favourable. The K_F and L values increase in order $3686_d < 3686_o < 3686$ as the P(V) adsorption increases. Based on the numerical values of L (Table 8), the sample 3686 has the highest adsorption affinity for P(V).

For a dilute solution of charged and uncharged adsorbates, the thermodynamic equilibrium constant of adsorption would be reasonably approximated by the Langmuir equilibrium constant K ($L \text{ mol}^{-1}$). When the equilibrium concentration is referred as the standard concentration, Langmuir isotherm constant K is nondimensional (Chatterjee & Woo, 2009). The relationship between the L and K can be written as: K ($L \text{ mol}^{-1}$) = $L \cdot M(P) \cdot 10^3$, where $M(P)$ is the molar mass of P(V). The adsorption equilibrium constant K is used to estimate the Gibbs free energy, $\Delta G^0 = -RT \ln K$. Based on data for Langmuir constants L from Table 8, the corresponding values of Gibbs free energy were calculated:

$$\Delta G_{298}^0(3686) = -23.28 \text{ kJ/mol,}$$

$$\Delta G_{298}^0(3686_o) = -21.89 \text{ kJ/mol.}$$

and

$$\Delta G_{298}^0(3686_d) = -20.57 \text{ kJ/mol}$$

The negative values of free energy change indicate that the adsorption process on the solid (terra rossa)/liquid (P(V)) interface is thermodynamically spontaneous. The higher negative value of ΔG_{298}^0 reflects a more energetically favourable adsorption (sample 3686).

The following aqueous and surface species dominate in the systems of hematite, kaolinite and P(V): H^+ , OH^- , $H_2PO_4^-$, HPO_4^{2-} , Mg^{2+} , Na^+ , $\equiv FeOH$, $\equiv FeOH_2^+$, $\equiv FePO_4H^-$, $\equiv FePO_4H_2^0$, $-SiOH$, $-Si-OH_2^+$, $Al-OH$ and $Al-OH_2^+$. The mechanism of adsorption of P(V) on the variety of active sites (Fe-oxides, kaolinite, illite) on the surface of the solid phase is complex. The strong sorption of P(V) might occur via displacement of coordinated surface hydroxyls ($\equiv Fe-OH + HPO_4^- \rightarrow \equiv Fe-PO_4^{2-} + H_2O$) and formation of mono and bidentate inner sphere surface complexes on hematite (Huang, 2004; Spiteri *et al.*, 2008). The proposed mechanism for retention of P(V) in soil by clay minerals is through a ligand exchange reaction with hydroxyl groups coordinated with the Al ions at the edge of crystals (Muljadi *et al.*, 1966).

TABLE 6. Trace elements contents (in ppm).

Sample	Ba	Co	Cr	Cu	Ga	Mo	Nb	Ni	Pb	Rb	Sr	Th	U	V	W	Y	Zn	Zr
3686	382	19	147	36	29	<5	29	79	46	180	95	30	<5	172	8	15	107	253
3687	315	16	189	35	23	5	24	85	34	128	67	19	<5	207	10	16	104	226
3688	263	21	167	42	32	<5	29	68	25	158	51	17	<5	245	<5	<5	68	122

Phosphate removal from wastewater by terra rossa

After 24 h of contact with the synthetic wastewater (Table 9), 29.9–32.6% (0.63–0.71 mg g⁻¹) of P(V) was removed in experiments with the original samples of terra rossa. The final pH values increased slightly from the initial value of 7.0. The P(V) removal by sample 3686 decreased significantly after removal of oxalate and dithionite extractable iron (25.9 and 19.9% or 0.56 and 0.43 mg g⁻¹, respectively). The treatment of sample 3686 was accompanied by differences in the final pH values when compared with the original sample. The P(V) removal by terra rossa was much higher than by natural sepiolites (Hrenovic *et al.*, 2010, 2012) or by natural bentonites (Hrenovic *et al.*, 2009a,b) which had a lower content of iron. The P(V) removal from wastewater was strongly correlated with the total Fe content in all terra rossa samples examined ($R^2 = 0.875$) as well as in samples 3686, 3686_o and 3686_d ($R^2 = 0.891$), suggesting that the iron content in terra rossa was the key factor controlling the P(V) removal from wastewater. In a complex aqueous medium competitive adsorption of P(V) and other anions onto terra rossa might occur. Therefore, the P(V) adsorption on terra rossa will vary with the

type of wastewater and may differ from that in the form of P(V) salt.

Immobilization of *A. junii* onto terra rossa and phosphate removal from wastewater

The pure culture of bacteria *A. junii* displayed typical multiplication and P(V) removal from synthetic wastewater (Table 9). In reactors with added terra rossa the majority of the bacteria were immobilized onto particles of material, while the minority remained in the supernatant as planktonic cells. The number of total bacteria and the multiplication of *A. junii*, as was indicated by the ratio of final/start number of bacteria (Table 9), suggest enhanced growth of bacteria in reactors with addition of terra rossa. Obviously the bacteria multiplied better when immobilized in biofilm, where the macro and micro nutrients present in terra rossa are available for stimulation of bacterial growth. The final pH values (Table 9) in reactors with terra rossa differed by up to 0.79 pH units from the reactor containing only *A. junii*. The possible negative influence of pH on the *A. junii* is not considered plausible, since these bacteria grow in the pH range 5–8 (Garrity *et al.*, 2005).

The number of immobilized bacteria was inversely correlated with the particle size of the

TABLE 7. Adsorption of P(V) by original and modified samples of terra rossa 3686 from solution of P(V) of different initial (Ca_o) concentration.

Sample Ca_o P(V) (mg L ⁻¹)	3686 — P(V) removed (%) —	3686 _o	3686 _d	3686 — Q P(V) (mg g ⁻¹) —	3686 _o	3686 _d
2.10	97.52	91.62	79.66	0.20	0.19	0.17
4.89	91.33	67.33	64.33	0.45	0.33	0.31
9.78	73.00	57.67	45.00	0.71	0.56	0.44
15.16	59.57	51.83	36.77	0.90	0.79	0.56
19.50	48.49	42.47	27.09	0.94	0.83	0.53
29.67	36.26	31.87	24.73	1.08	0.94	0.73
49.88	27.45	24.84	20.59	1.37	1.24	1.02

TABLE 8. Freundlich and Langmuir isotherm parameters obtained from the equations of adsorption isotherms for the adsorption of P(V) by original and modified samples of terra rossa sample 3686. R^2 is the coefficient of determination.

Freundlich linearized form: —— $\ln(Q) = (n)^{-1} \ln(C) + \ln(K_F)$ ——				Langmuir linearized form: —— $C(Q)^{-1} = (Q_{\max})^{-1} C + (Q_{\max}L)^{-1}$ ——			
Sample	3686	3686 _o	3686 _d	Sample	3686	3686 _o	3686 _d
$k = (n)^{-1}$	0.28	0.36	0.37	$k = (Q_{\max})^{-1}$	0.001	0.001	0.001
$l = \ln(K_F)$	6.24	5.82	5.46	$l = (Q_{\max}L)^{-1}$	0.002	0.004	0.007
$n = (k)^{-1}$	3.59	2.78	2.69	$Q_{\max}(\text{mg g}^{-1})^{-1} = (k)^{-1}$	1.43	1.25	1.11
$K_F = e^l$	0.51	0.34	0.23	$L(\text{Lmg}^{-1})^{-1} = (l \cdot Q_{\max})^{-1}$	0.39	0.22	0.13
$Q(49.88)$	1.39	1.24	0.92	$Q(49.88)$	1.33	1.12	0.93
R^2	0.99	0.98	0.98	R^2	0.98	0.97	0.90

support materials (Hrenovic *et al.*, 2009a). Since the terra rossa mainly consisted of particles <100 μm , it represents a promising substrate for the immobilization of bacteria. The number of immobilized *A. junii* bacteria onto sample 3687 was comparable with the numbers of *A. junii* immobilized onto natural bentonites (4.79×10^9 CFU g^{-1} and 5.82×10^9 CFU g^{-1}) and natural sepiolites (5.6×10^9 CFU g^{-1}) (Hrenovic *et al.*, 2009a,b, 2010, 2012), while for sample 3688 they were slightly higher. The number of immobilized *A. junii* bacteria onto original and treated terra rossa samples 3686 was the highest among all carriers of *Acinetobacter* species reported in the literature. The numbers of immobilized *A. junii* bacteria onto samples 3686 and 3686_d were comparable to the number of *P. putida* adsorbed onto montmorillonite (3.2×10^{10} cells g^{-1}) and kaolinite (4.1×10^{10} cells g^{-1}) (Jiang *et al.*, 2007), while for sample 3686_o they were significantly higher.

The absence of correlation between the iron content and number of immobilized bacteria suggests that the iron content was not the important parameter controlling immobilization of bacteria onto terra rossa. The reason for the high number of immobilized *A. junii* onto original sample 3686 can be due to the higher content of potassium and higher amount of illitic material, especially in the <0.2 μm fraction, as compared to samples 3687 and 3688 (Tables 4 and 5). The increased number of the immobilized bacteria onto sample 3686_o may be attributed to a significant reduction of particle size after acid ammonium oxalate treatment. In an ongoing study (Durn *et al.*, unpublished data) on surface physico-chemical properties of terra rossa

and calcomelanosol developed on hard limestone, samples treated with ammonium oxalate displayed significant increase of the clay fraction content (especially the <0.45 μm fraction), specific surface area (SSA) and cation exchange capacity (CEC) as compared to the original terra rossa sample. This was accompanied by a reduction of microaggregate size (from <2000 nm to <400 nm in diameter), indicating that clays were aggregated by poorly crystalline Fe oxides (Fe_o). The ratio of immobilized and planktonic bacteria in reactors (Table 9) confirmed that sample 3686 is the best support material among the original samples of terra rossa and sample 3686_o is an excellent sample for bacterial immobilization. To our knowledge, the number of 1.34×10^{11} CFU g^{-1} immobilized onto sample 3686_o is the highest number of immobilized bacteria reported in the literature so far. However, the removal of the oxalate extractable iron from terra rossa would not be cost efficient when used on a large scale. For commercial use, the original samples of terra rossa could serve as good support materials for the immobilization of bacteria.

The P(V) removal in reactors with *A. junii* and terra rossa was significantly higher than in corresponding reactors without bacteria (Table 9). The log CFU of total bacteria in reactors showed highly positive correlation with the percentage of P(V) removal from wastewater ($R^2 = 0.913$), suggesting that the bacterial biomass was an important factor for overall P(V) removal from wastewater. The contribution of bacteria in the P(V) removal from wastewater ranged from 20.2 to 36.6%. In reactors containing the *A. junii* and terra rossa, P(V) was removed from wastewater by

TABLE 9. Performance of reactors containing *A. junii* only, *A. junii* with addition of terra rossa, and terra rossa only after 24 h of incubation.

Reactor	P(V) removed (%)	Final pH	Immobilized cells (10 ¹⁰ CFU g ⁻¹)	Planktonic cells (10 ⁸ CFU mL ⁻¹)	Total cells (10 ⁸ CFU mL ⁻¹)	Immobilized/ planktonic cells	Final/start cells
<i>A. junii</i>	21.8±0.3	7.29±0.02	—	0.63±0.02	0.63±0.02	—	8±0
3686 <i>A. junii</i>	55.4±0.7	7.89±0.02	2.47±1.25	2.86±0.08	5.32±1.17	86±41	73±14
3686 _o <i>A. junii</i>	62.5±1.3 ^B	7.84±0.02 ^B	13.43±1.58 ^B	0.17±0.06 ^B	13.60±1.55 ^B	7935±392 ^B	197±27 ^B
3686 _d <i>A. junii</i>	40.5±1.0 ^B	8.08±0.02 ^B	2.71±0.16	1.12±0.12 ^B	3.82±0.04 ^B	245±41 ^B	72±3
3687 <i>A. junii</i>	51.4±0.6	7.90±0.02	0.56±0.02	2.13±0.10	2.68±0.08	26±2	52±1
3688 <i>A. junii</i>	53.1±0.7	7.93±0.02	0.99±0.06	2.67±0.24	3.66±0.18	37±6	52±3
3686	32.6±0.3 ^A	7.86±0.02	—	—	—	—	—
3686 _o	25.9±0.7 ^{A,B}	6.23±0.02 ^{A,B}	—	—	—	—	—
3686 _d	19.9±0.7 ^{A,B}	7.22±0.02 ^{A,B}	—	—	—	—	—
3687	31.2±0.3 ^A	7.78±0.02 ^A	—	—	—	—	—
3688	29.9±0.7 ^A	7.79±0.02 ^A	—	—	—	—	—

[c₀ CFU (10⁶ mL⁻¹)] = 6.56±1.02; [c₀ P-PO₄ (mg L⁻¹)] = 21.7±0.4, significantly different values: ^A Compared to corresponding reactor with bacteria; ^B Compared to untreated sample 3686.

simultaneous adsorption onto terra rossa and accumulation of poly-P(V) inside cells of *A. junii*.

Although the use of P(V)-accumulating bacteria could remove large amounts of P(V) from wastewater, the rate of bacterial P(V) removal is significantly lower at temperatures below 20°C (Marklund, 1993). Terra rossa has great potential for P(V) adsorption from wastewater and immobilization of P(V)-accumulating bacteria. Therefore, in the wastewater treatment plants operating in moderate and cold climates terra rossa can serve as an adsorbent of P(V) and a pool of P(V)-accumulating bacteria, which will become active at higher temperatures.

CONCLUSIONS

Terra rossa from Croatia has been found to be a suitable substrate for the improvement of biological P(V) removal from wastewater. It meets the requirements of an ideal material as the carrier of bacteria and sorbent of P(V) from wastewater because it has high affinity for immobilization of P(V)-accumulating bacteria, high P(V) adsorption capacity in the complex medium, it is inert, nontoxic, environmentally friendly, easily available, inexpensive and useful for soil improvement after saturation with P(V).

ACKNOWLEDGMENTS

This research was supported by the Ministry of Science, Education and Sports of the Republic of Croatia (project nos. 119-1191155-1203 and 195-1953068-2704).

REFERENCES

- Altay I. (1997) Red Mediterranean soils in some karstic regions of Taurus mountains, Turkey. *Catena*, **28**, 247–260.
- Banerjee A. & Merino E. (2011) Terra rossa genesis by replacement of limestone by kaolinite. III. Dynamic quantitative model. *The Journal of Geology*, **119**, 259–274.
- Bech J., Rustullet J., Garigo J., Tobias F.J. & Martinez R. (1997) The iron content of some red Mediterranean soils from Northeast Spain and its pedogenic significance. *Catena*, **28**, 211–229.
- Blume H.P. & Schwertmann V. (1969) Genetic evaluation of profile distribution of Al, Fe and Mn oxides. *Proceedings - Soil Science Society of America*, **33**, 438–444.

- Boero V. & Schwertmann U. (1989) Iron oxide mineralogy of terra rossa and its genetic Implications. *Geoderma*, **44**, 319–327.
- Boero V., Premoli A., Melis P., Barberis E. & Arduino E. (1992) Influence of climate on the iron oxide mineralogy of terra rossa. *Clays and Clay Minerals*, **40**, 8–13.
- Brindley G.W. & Brown G. (1980) *Crystal Structures of Clay Minerals and their X-ray Identification*. Monograph 5, Mineralogical Society, London, 495 pp.
- Bronger A. & Bruhn-Lobin N. (1997) Paleopedology of terrae rossae-Rhodoxeralfs from Quaternary calcarenites in NW Morocco. *Catena*, **28**, 279–295.
- Brown G. (1961) *The X-ray Identification and Crystal Structures of Clay Minerals*. Mineralogical Society, London, 544 pp.
- Chatterjee S. & Woo S.H. (2009) The removal of nitrate from aqueous solutions by chitosan hydrogel beads. *Journal of Hazardous Materials*, **164**, 1012–1018.
- Davis T.A., Volesky B. & Mucci A. (2003) A review of the biochemistry of heavy metal biosorption by brown algae. *Water Research*, **37**, 4311–4330.
- Douglas L.A. (1989) Vermiculites. Pp. 634–674 in: *Minerals in Soil Environments* (J.B. Dixon & S.B. Weed, editors). Soil Science Society of America, Madison, Wisconsin.
- Duchaufour P. (1982) *Pedology: Pedogenesis and Classification*. Allen and Unwin, London, 448 pp.
- Durham D.R., Marshall L.C., Miller J.G. & Chmurny A.B. (1994) Characterization of inorganic biocarriers that moderate system upsets during fixed-film biotreatment processes. *Applied and Environmental Microbiology*, **60**, 3329–3335.
- Durn G., Ottner F. & Slovenec D. (1999) Mineralogical and geochemical indicators of the polygenetic nature of terra rossa in Istria, Croatia. *Geoderma*, **91**, 125–150.
- Durn G., Slovenec D. & Covic M. (2001) Distribution of iron and manganese in terra rossa from Istria and its genetic implications. *Geologia Croatica*, **54**, 27–36.
- Durn G., Aljinovic D., Crnjakovic M. & Lugovic B. (2007) Heavy and light mineral fractions indicate polygenesis of extensive terra rossa soils in Istria, Croatia. Pp. 701–737 in: *Heavy Minerals in Use* (M.A. Mange & D.T. Wright, editors). Developments in Sedimentology, **58**, Elsevier.
- FAO (1974) *Soil Map of the World*, 1:5 Mill., Volume 1. Legend, Unesco, Paris.
- Garcia-Gonzales M.T. & Recio P. (1988) Geochemistry and mineralogy of the clay fraction from some Spanish terra rossa. *Agrochimica*, **32**, 161–170.
- Garrity G.M., Brenner D.J., Krieg N.R. & Staley J.T. (2005) *Bergey's Manual of Systematic Bacteriology*, **2**, Part B. Springer, New York, 425–437.
- Hrenovic J., Ivankovic T. & Tibljas D. (2009a) The effect of mineral carrier composition on phosphate-accumulating bacteria immobilization. *Journal of Hazardous Materials*, **166**, 1377–1382.
- Hrenovic J., Rozic M., Ivankovic T. & Farkas A. (2009b) Biosorption of phosphate from synthetic wastewater by biosolids. *Central European Journal of Biology*, **4**, 397–403.
- Hrenovic J., Ivankovic T., Tibljas D., Kovacevic D. & Sekovanic L. (2010) Sepiolite as carrier of the phosphate-accumulating bacteria *Acinetobacter junii*. *Applied Clay Science*, **50**, 582–587.
- Hrenovic J., Zigovecki Gobac Z. & Bermanec V. (2012) Occurrence of sepiolite in Croatia and its application in phosphate removal from wastewater. *Applied Clay Science*, **59-60**, 64–68.
- Huang X. (2004) Intersection of isotherms for phosphate adsorption on hematite. *Journal of Colloid and Interface Science*, **271**, 296–307.
- Jiang D., Huang Q., Cai P., Rong X. & Chen W. (2007) Adsorption of *Pseudomonas putida* on clay minerals and iron oxide. *Colloids and Surfaces B: Biointerfaces*, **54**, 217–221.
- Johns W.D., Grim R.E. & Bradley W.F. (1954) Quantitative estimations of clay minerals by diffraction methods. *Journal of Sedimentary Petrology*, **24**, 242–251.
- Li R., Kelly C., Keegan R., Xiao L., Morrison L. & Zhan X. (2013) Phosphorus removal from wastewater using natural pyrrhotite. *Colloids and Surfaces A: Physicochemical and Engineering Aspects*, **427**, 13–18.
- Limousin G., Gaudet J.P., Charlet L., Szenknect S., Barthes V. & Krimissa M. (2007) Sorption isotherms: a review on physical bases, modelling and measurement. *Applied Geochemistry*, **22**, 249–275.
- Marklund S. (1993) Cold climate sequencing batch reactor biological phosphorus removal – results 1991–92. *Water Science & Technology*, **28**, 275–282.
- Mehra O.P. & Jackson M.L. (1960) Iron oxides removal from soils and clays by a dithionite-citrate-bicarbonate system buffered with sodium bicarbonate. *7th National Conference on Clays and Clay Minerals*, **7**, 317–327.
- Merino E. & Banerjee A. (2008) Terra rossa genesis, implications for karst, and eolian dust: A geodynamic thread. *The Journal of Geology*, **116**, 62–75.[GEC1]
- Miko S., Durn G. & Prohic E. (1999) Evaluation of terra rossa geochemical baselines from Croatian karst regions. *Journal of Geochemical Exploration*, **66**, 173–182.
- Miko S., Halamic J., Peh Z. & Galovic L. (2001) Geochemical baseline mapping of soils developed on diverse bedrock from two regions in Croatia. *Geologia Croatica*, **54**, 53–118.
- Miko S., Durn G., Adamcova R., Covic M., Dubikova M., Skalsky R., Kapelj S. & Ottner F. (2003) Heavy

- metal distribution in karst soils from Croatia and Slovakia. *Environmental Geology*, **45**, 262–272.
- Moore D.M. & Reynolds R.C. (1989) *X-ray diffraction and the Identification and Analysis of Clay Minerals*. Oxford University Press, Oxford, 326 pp.
- Moresi M. & Mongelli G. (1988) The relation between the terra rossa and the carbonate-free residue of the underlying limestones and dolostones in Apulia, Italy. *Clay Minerals*, **23**, 439–446.
- Mortula M., Gibbons M. & Gagnon G.A. (2007) Phosphorus adsorption by naturally occurring materials and industrial by-products. *Journal of Environmental Engineering and Science*, **6**, 157–164.
- Muljadi D., Posner A.M. & Quirk J.P. (1966) The mechanism of phosphate adsorption by kaolinite, gibbsite and pseudoboehmite. *European Journal of Soil Science*, **17**, 230–237.
- Munsell Soil Color Charts (1994) Macbeth Division of Kollmorgen Instruments, New Windsor, New York, USA.
- Range K.J., Range A. & Weiss A. (1969) Fire-clay type kaolinite or fire-clay mineral? Experimental classification of kaolinite-halloysite minerals. *Proceedings of the 3rd International Clay Conference, Tokyo*, **1**, 3–13.
- Riedmüller G. (1978) Neoformations and transformations of clay minerals in tectonic shear zones. *Tschermaks Mineralogische und Petrographische Mitteilungen (TMPM)*, **25**, 219–242.
- Ruhlicke G. & Niederbudde E.A. (1985) Determination of layer-charge density of expandable 2:1 clay minerals in soils and loess sediments using the alkylammonium method. *Clay Minerals*, **20**, 291–300.
- Sawahla M.F., Peralta-Videa J.R., Romero-Gonzales J. & Gardea-Torresdey J.L. (2006) Biosorption of Cd(III), and Cr(VI) by saltbush (*Atriplex canescens*) biomass: thermodynamic and isotherm studies. *Journal of Colloid and Interface Science*, **300**, 100–104.
- Schwertmann U. (1964) Differenzierung der Eisenoxide des Bodens durch photochemische Extraktion mit saurer Ammoniumoxalat-lösung. *Z. Pflanzenernähr. Bodenkund*, **105**, 194–202.
- Schwertmann U. & Taylor R.M. (1989) Iron oxides. Pp. 379–438 in: *Minerals in Soil Environments*, 2nd edition (J.B. Dixon & S.B. Weed, editors). Soil Science Society of America Book Series, **1**.
- Schwertmann U., Murad E. & Schulze D.G. (1982) Is there Holocene reddening (hematite formation) in soils of oxic temperate areas? *Geoderma*, **27**, 209–223.
- Sidat M., Bux F. & Kasan H.C. (1999) Phosphate accumulation by bacteria isolated from activated sludge. *Water SA*, **25**, 175–179.
- Soil Survey Staff (1975) *Soil taxonomy: a basic system of soil classification for making and interpreting soil surveys*. USDA Handbook No.436, U.S. Government Printing Office, Washington, D.C.
- Sondi I. & Pravdic V. (1998) The colloid and surface chemistry of clays in natural water. *Croatica Chemica Acta*, **71**, 1061–1074.
- Spiteri C., Van Cappellen P. & Regnier P. (2008) Surface complexation effects on phosphate adsorption to ferric iron oxyhydroxides along pH and salinity gradients in estuaries and coastal aquifers. *Geochimica et Cosmochimica Acta*, **72**, 3431–3445.
- Środoń J. (1984) X-ray powder diffraction identification of illitic materials. *Clays and Clay Minerals*, **32**, 337–349.
- Środoń J. & Eberl D.D. (1984) Illite. Pp. 495–544 in: *Micas* (S.W. Bailey, editor). *Reviews in Mineralogy*, **13**. Mineralogical Society of America.
- Torrent J. (1995) *Genesis and Properties of the Soils of the Mediterranean Regions*. Dipartimento di Scienze Chimico-Agrarie, Università degli Studi di Napoli Federico II, 111 pp.
- Tributh H. (1991) Notwendigkeit und Vorteile der Aufbereitung von Boden und Lagerstätten tonen. Pp. 29–33 in: *Identifizierung und Charakterisierung von Tonmineralen. Berichte der Deutschen Ton und Tonmineralogruppe, Giessen und Schloss Rauischholzhausen, 10-12 Mai 1989* (H. Tributh & G. Lagaly, editors).
- Tributh H. & Lagaly G. (1986) Aufbereitung und Identifizierung von Boden und Lagerstätten tonen, I. Aufbereitung der Proben im Labor. *GIT Labor-Fachzeitschrift*, **30**, 524–529.
- Wang C., Guo W., Tian B., Pei Y. & Zhang K. (2011) Characteristics and kinetics of phosphate adsorption on dewatered ferric-alum residuals. *Journal of Environmental Science and Health, Part A Toxic/Hazardous Substances and Environmental Engineering*, **46**, 1632–1639.